Electromechanical Modeling of MEMS Resonators with MOSFET Detection

N. Abelé*,**, V. Pott*, K. Boucart*, F. Casset***, K. Séguéni**, P. Ancey** and A.M. Ionescu*
* Swiss Federal Institue of Technology, STI-LEG, Lausanne 1015, Switzerland
** ST Microelectronics, Crolles, France
*** CEA-LETI, Grenoble, France

ABSTRACT

Several studies of resonating MEMS structures using the suspended gate of a MOS transistor for the detection of the displacement have shown that this can be an accurate technique for precise measurement. This article reports on the analytical modeling of Resonant Gate Transistor (RGT) based on the so-called Suspended-Gate MOSFET (SG-MOSFET). The model includes a dynamic mechanical model of a fixed-fixed beam resonator as well as a MOSFET model that is continuous from depletion to inversion. It was found that the RSG-MOSFET gives a significantly much higher output current than a conventional metal-metal capacitive detection for channel length smaller than a critical value that is discussed in a case study. Therefore, MOSFET detection appears more suitable for highly scaled MEMS resonators extending the scalability of this class of resonators in general.

Keywords: RSG-MOSFET, dynamic mechanical model, MOSFET transistor, MEMS resonator, RGT

1 INTRODUCTION

MEMS devices dedicated to RF signal processing are very attractive for wireless communication because of their low power consumption, small size and potential for CMOS co-integration. As these components are scaled down and therefore increasingly compatible with MOSFET fabrication, there is a strong need for co-simulation of the mechanical and electrical behavior. The main displacement detection technique used in micro-resonator devices is a metal-metal capacitive type. At that scale, however, the displacement of a high frequency MEMS structure is so small that the transmitted signal has a very low amplitude. Capacitive type devices have therefore limitations in terms of output signal level because of the high parasitic capacitive coupling that can overload the useful signal coming from the structure displacement.

On that base, the MOSFET appears to be a good technique for detecting the resonator vibrations. According to [1], the use of a MOSFET can be preferable for circuit applications due to its potential for high resolution at high frequency. Even though bulk acoustic resonators like disk resonators described in [2] can achieve resonant frequencies up to 1.15GHz with very high quality factors, a *fixed-fixed* beam resonator was preferred in this work for the analytical modeling, as its mechanical behavior is well understood and the related displacement can be calculated accurately.

This paper presents the electrical and mechanical results of a bulk RSG-MOSFET that is based on the analysis of the non-linear mechanical oscillation of a resonator [3] coupled with the electrical SG-MOSFET [4] and the RGT [5] equations.

2 ELECTRO-MECHANICAL MODEL

The investigated RSG-MOSFET is composed of an anchored suspended gate transistor (see Fig. 1). The gate is suspended over the transistor channel. The resonator is electrostatically actuated by application of AC and DC voltages on the beam resulting in a vertical vibration. The natural beam frequency is calculated from its dimensions and geometry. For an input signal applied on the gate at the natural frequency, the resonance occurs. Beam resonance is characterized by large deflection amplitude which is limited by the mechanical damping of the structure. The beam displacement modulates the capacitance sensed by the MOSFET and produces an alternative drain current component.

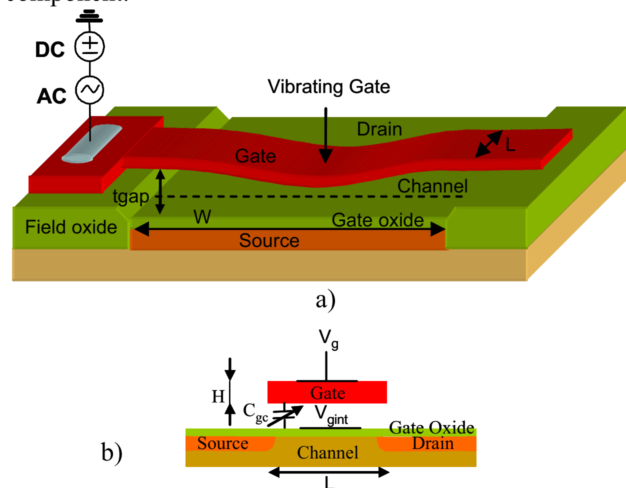

Fig. 1: a) 3D view and b) cross section of a RSG-MOSFET based on a vibrating fixed-fixed beam.

The mechanical vibration of the beam is characterized by the following Duffing equation (1) for large amplitude displacement of a non-linear oscillator.

$$m\ddot{y} + c\dot{y} + ky + k_{dyn}y^3 = F_{elec} \quad (1)$$

The damping coefficient c of the beam represents the losses mainly due to the air damping of the structure and to

heat dissipation. The rigidity of the structure is calculated from its geometry and dimensions and must include the structural layer stress σ_{stress}. For a tensile stress, the stiffness can be expressed as:

$$k = \frac{192EI}{L^3} + 8\sigma_{stress}(1-\upsilon)W\frac{H}{L} \quad (2)$$

$$I = \frac{WH^3}{12} \quad (3)$$

The displacement non-linearity of the resonator is characterized by a dynamic rigidity k_{dyn} coefficient [6]. This factor is related to the stretching of the beam, and therefore its stiffening for large displacement. It can be calculated, according to [6], and depends on the Young's modulus of the beam material, the beam length W, width L and thickness H:

$$k_{dyn} = \frac{\pi^4 EWH}{8L^3} \quad (4)$$

The dynamic behavior of the vibrating beam, as a function of the dynamic rigidity and electrostatic force is also very dependent to the damping factor c, related to the quality factor Q by the equation (5):

$$c = \frac{\omega m}{Q} \quad (5)$$

In the case of an RSG-MOSFET, the electrostatic force F_{elec} varies with the gate voltage but also with the surface potential of the MOSFET channel and is expressed as:

$$F_{elec} = \frac{1}{2}\frac{\varepsilon_0 WL}{(t_{gap} - y)^2}V_{g\,int}^2(t) \quad (6)$$

$$V_{g\,int} = \frac{\left(V_{DC} + V_{AC}\cos(\omega t)\right)}{\left(1 + \frac{C_{gc}}{C_{gap}}\right)} \quad (7)$$

The electrical field created by the applied gate voltage is lowered at the MOSFET channel interface due to the air gap C_{gap} and gap-to-substrate C_{gc} capacitances. The electrostatic potential between gate and substrate changes from V_g-V_{bulk} to V_g-ψ_S with ψ_S the channel surface potential ($\psi_S > V_{bulk}$). The pull-in voltage, which is the limiting voltage that can be applied on the gate before the beam collapses, is modified for an RSG-MOSFET. For the capacitive type resonator, the pull-in voltage V_{pi} is expressed as:

$$V_{pi} = \sqrt{\frac{8k}{27\varepsilon_0 WL}t_{gap}^3} \quad (8)$$

For the RSG-MOSFET the equation becomes:

$$V_{pi_MOS} = \sqrt{\frac{8.k_{dyn}\left(1 + \frac{C_{gc}}{C_{gap}}\right)^2 t_{gap}^3}{27\varepsilon_0 A}} \quad (9)$$

The V_{pi} dependence on the gate voltage, V_g, is described in Fig. 2, clearly showing that the structure collapses at higher voltage for an RSG-MOSFET than for a metal-metal resonator. The resulting electrostatic forces are lower on the RSG-MOSFET for the same V_g and the beam amplitude is smaller.

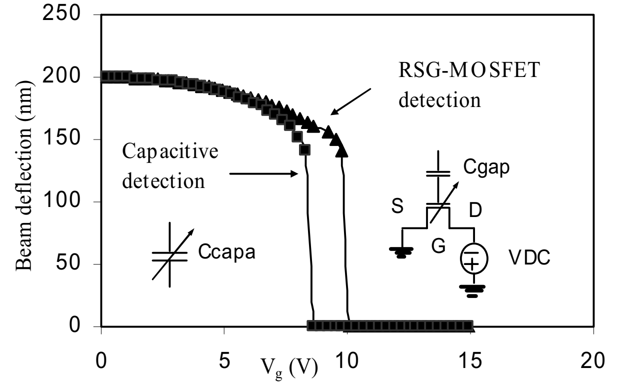

Fig. 2: Pull-in voltage for capacitive and RSG-MOSFET using fixed-fixed beam resonator architecture working at low resonance frequency for t_{gap} = 200nm (1.75 MHz).

The electrical modeling of the RSG-MOSFET is a long-channel MOSFET model. It is based upon a continuous expression of weak, moderate and strong inversion of the gate-to-channel capacitance C_{gc}. The air gap t_{gap} and the channel oxide t_{ox} work as a capacitive divider for the applied gate voltage V_g, so that an intrinsic voltage V_{gint} acts on the MOSFET channel as expressed in (7). The gate-to-channel capacitance is a function of the gate oxide, inversion and depletion layer capacitances, C_{ox}, C_{inv} and $C_{depletion}$, as in:

$$C_{gc}(V_{g\,int}) = \frac{\partial Q_{inv}}{\partial V_{g\,int}} = \frac{C_{ox}C_{inv}}{C_{ox} + C_{inv} + C_{depletion}} \quad (10)$$

This capacitance is calculated from the beam deflection and the surface channel potential. The drain-source current I_{DS} is derived from these equations with the inversion layer charge Q_{inv} of the channel as expressed in (11) and (12).

$$Q_{inv} = \int_{v_s}^{v_d} C_{gc}(V_{g\,int})dV_{g\,int} \quad (11)$$

$$I_{DS} = \mu_n \cdot C_{ox} \cdot \frac{W}{L}\int_{V_S}^{V_D} -\frac{Q_{inv}}{C_{ox}}dV \quad (12)$$

The output drain current is modulated by the beam displacement induced by the gate AC voltage but also depends on the applied gate dc voltage. The non-linearity of the transistor and the displacement due to the electrostatic actuation work together to increase the output signal amplitude peak. The quality factor of the device corresponds to some extent to the sharpness of the signal peak and is therefore increased due to the transistor gain.

The fixed-fixed beam has a deflection shape as presented in Fig. 3. For modeling purposes, the beam length is divided into N (integer) sections.

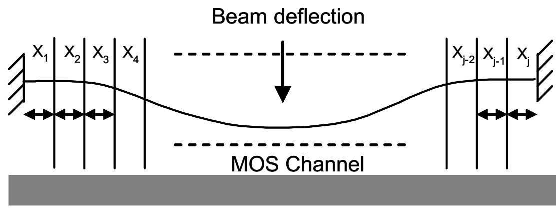

Figure 3: Schematic of the beam deflection shape for an electrostatic actuation.

The total gate-to-substrate capacitance C_{gc} is then calculated as the sum of the parallel capacitances of the N sections:

$$C_{gc} = \sum_{y=X_i}^{X_n} C_{gc}(y) \tag{13}$$

For each section, the C_{gc} is calculated accordingly to the gap size and the electrostatic field acting in that region. The total output current I_{DS} is then calculated according to equations (11) and (12). Prediction of the electrical parameters (ΔC_{gc} , g_m, ΔI_{DS}) of the RSG-MOSFET can be carried out from the model.

3 DESIGN OF THE RSG-MOSFET

The electro-mechanical RSG-MOSFET model is shown to be accurate in static operation (see Fig. 4) by comparing to results from the operational device described in [7]. The device is a thin-film transistor (TFT) with a doped polysilicon suspended gate over a 500nm air gap. The anchor geometry is similar to Fig. 1. The RSG-MOSFET electrical behavior fits perfectly the measured one in all MOSFET regions.

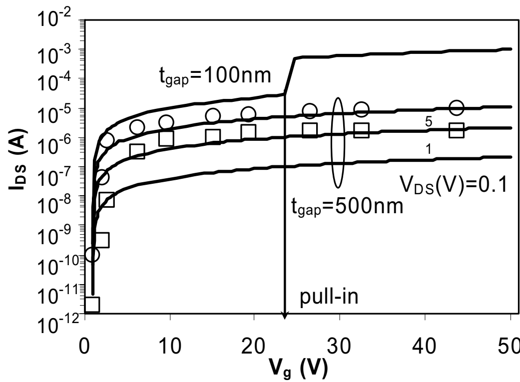

Figure 4: Comparison between simulated and experimental results from [7] for a fixed-fixed beam structure for various drain-source voltages V_{ds}.

The validity in static operation can be extended to dynamic operation for both small and large signal amplitude V_{AC} analysis. RSG-MOSFET design is based on the maximum output I_{DS} current with the largest peak-to-peak amplitude. Simulations of this device for a 100nm gap have been performed to show the pull-in effect of the structure at 23V. For proper design of the RSG-MOSFET, trade-offs between the resonator dimensions, the resonance frequency, the gap size, the gate voltage and the gate oxide thickness must be made in order to maximize the output current. The RSG-MOSFET capacitive divider as expressed in (6) varies with the gate oxide thickness. The variation of V_{gint} as a function of V_g for various oxide thicknesses is shown in Fig. 5. It is composed of a linear part for which the V_{gint} equals V_g, a nearly-flat one that corresponds to the MOS strong inversion settling and a pull-in section. Due to the low dielectric constant of the air gap compared to the silicon dioxide (e_{ox} = 3.9), the intrinsic voltage stays low (V_{gint} = 0.79 to 1.19V for t_{ox} between 5nm and 50nm) when V_g is close to the pull-in voltage. On this specific device the V_{gint} is nearly linear to V_g up to 0.63V for a 5nm oxide and to 1.04V for a 50nm oxide.

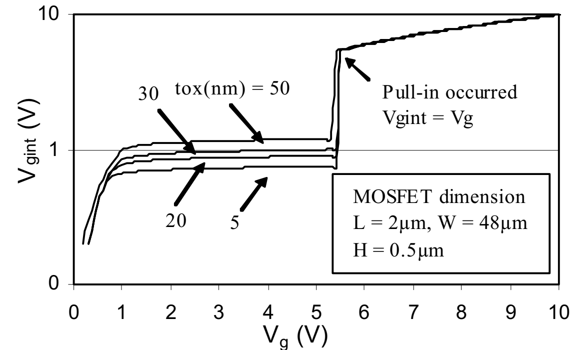

Figure 5: Simulated intrinsic gate voltage V_{gint} curves vs. gate voltage V_g for various oxide thicknesses.

The beam spring constant k also affects on the resonator behavior. A low k is needed for high deflection amplitude (large signal modulation) but a high k is required for high resonant frequency. Maximum output current I_{DS} for RSG-MOSFET detection is attained with a smaller beam, corresponding to a short channel transistor with large W whereas for capacitive detection a large area is needed. The current flowing through metallic plates is expressed as:

$$I_{capa} = V_{DC} \frac{d(\delta C_{metal-metal})}{dt} + C_{metal-metal} \frac{dv_{AC}}{dt} \tag{13}$$

Total output I_{DS} peak current for the RSG-MOSFET and capacitive detection for various beam widths are presented in Fig. 6.

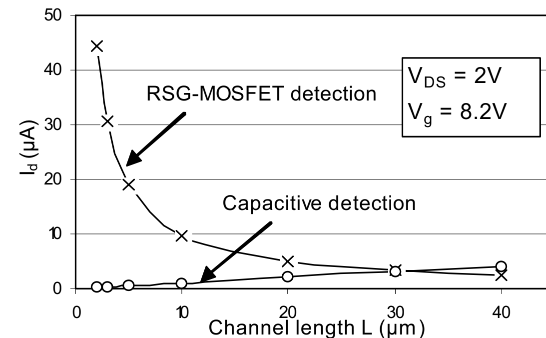

Figure 6: Comparison of the simulated peak current for capacitive and MOSFET detection for various beam widths at 1.75MHz.

RSG-MOSFET detection is then useful for a beam width lower than 30µm. The output current increases exponentially while reducing the beam width for an RSG-MOSFET whereas for capacitive detection, the current grows linearly for increasing beam width. Therefore, for a high frequency resonator around 350MHz (dimensions of the beam of W/L = 3.9µm/1µm with 600nm thickness), it is much recommended to use an RSG-MOSFET detection than a capacitive one, resulting in very significant gain in terms of output current level (see Fig. 7). The large amplitude non-linearity can be noticed at the peak due to the non-linear electrostatic actuation.

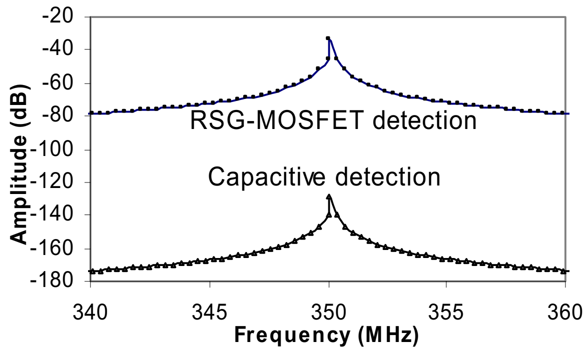

Figure 7: Output signal amplitude for a 350MHz silicon resonator for a 20V actuation voltage with Q = 5000.

High power handling capability and therefore large volume structures were shown to be needed [8] for capacitive detection in order to have a measurable output signal. A very large beam for capacitive measurement or thick beams for the RSG-MOSFET can be used. However, the higher output current level for RSG-MOSFET detection reduces the need for large volume structures. Amplitude peak-to-peak variation is also higher than for a capacitive detection and more suitable for circuit integration.

4 Noise in the RSG-MOSFET

The mechanical noise equations from [9] and [10] due to the resonating beam and the electrical noise due to MOS transistor behavior have been added to the model. Mechanical noises, when the resonator is in a perfect vacuum, are mainly *temperature fluctuations, Brownian and Johnson noise*. The temperature fluctuation noise comes from the heat exchange at the resonator surface and the thermal conduction at the interface with the environment. Mechanical Johnson noise is the noise due to random motion of charge in the beam that generates random voltage across the beam. This noise is frequency dependent. The electrical thermal noise coming from the MOSFET is the main noise source acting on the device. The RSG-MOSFET can be considered as a large channel transistor and the other noises acting usually on small channels can be neglected. Corresponding noise spectral density is presented (see Table 1) for comparing the influence of the noise sources for micro-scaled resonators.

Noise type	Noise spectral density (V^2/Hz)
Thermal mechanical	$2.48*10^{-14}$
Brownian	$3.94*10^{-15}$
Johnson	$5.62*10^{-15}$
Thermal electrical	$1.16*10^{-14}$

Table 1: Mechanical and electrical noise spectral density of a RSG-MOSFET at 350MHz.

For circuit design and modeling applications the associated voltage and current sources due to electrical and mechanical noise are needed in order to use them in a loop for circuit simulation.

5 CONCLUSION

A micromechanical dc/ac model for MEMS resonators based on a vibrating suspended beam and using a MOSFET transistor for signal detection was proposed and validated. Unlike previous models, we continuously cover all transistor operating regions and take into account mechanical non-linearities of the deflecting beam. We have demonstrated that MOSFET detection offers increased peak current compared to conventional capacitive detection and is particularly well suited for scaled resonators (resonant frequencies higher than 100MHz).

REFERENCES

[1] A. Weinert, G. I. Anderson, “High resolution resonant double gate transistor for oscillating structures”, S&A, 2000, A. 90 pp.20-30.
[2] J.Wang et al., “1.156GHz self-aligned vibrating micromechanical disk resonator”, IEEE Trans. On Ultras., Ferroelec. and Freq. Ctr., Vol.51, No.12, 2004
[3] S. Timoshenko, D.H. Young, W.Weaver, “Vibration problems in engineering”, John Wiley and Sons, 1974
[4] A.M.Ionescu, V.Pott, R.Fritschi and al., “Modeling and design of a low-voltage SOI suspended-gate MOSFET with a metal-over-gate architecture”, ISQED'02.
[5] H.C.Nathanson, W.E.Newell, R.A.Wickstrom, J.R.Davis Jr., “The resonant gate transistor”, IEEE Trans. on Electron Devices, 1967, Vol. ED-14,No.3.
[6] G. M. Rebeiz, “RF MEMS, Theory, design and technology”, Wiley, 2003.
[7] H. Mahfoz-Kotb et al.,” Air gap polycristalline silicon thin film transistors for fully integrated sensors”, IEEE EDL, Vol.24, No.3, 2003
[8] Y.-W. Lin, S. Lee, Z. Ren, C.T.-C. Nguyen, “Serie-resonant micromechanical resonator oscillator”, 2003
[9] A.N. Cleland, M.L. Roukes, “Noise in nanomechanical resonators”, J.Appl. Phys., Vol.92, No.5, pp.2758, 2002
[10] J.R. Vig, Y. Kim, “Noise in Micromechanical system resonators”, IEEE Trans. On ultr. and freq. control, 1999, Vol.46, No.6